

Galvanic Corrosion of Aluminum Alloy (Al2024) and Copper in 1.0 M Nitric Acid

Ahmed Y. Musa*, Abu Bakar Mohamad, Abdul Amir H. Kadhum, Eng Pei Chee,

Department of Chemical and Process Engineering, Faculty of Engineering and Built Environment, Universiti Kebangsaan Malaysia, Bangi, 43600, Selangor, Malaysia.

*E-mail: ahmed.musa@ymail.com; ahmedym@eng.ukm.my

Received: 26 July 2011 / Accepted: 11 September 2011 / Published: 1 October 2011

The corrosion behaviors of aluminum alloy (Al2024) and copper in 1.0 M nitric acid solution at different temperatures were investigated using electrochemical impedance spectroscopy (EIS) and potentiodynamic polarization (PDP) methods. The galvanic behavior of coupled metals was also studied using zero resistance ammetry (ZRA) method. The effect of temperature was explained by application of Arrhenius and transition state theory equations. Thermodynamic parameters of activation energy (E_a), enthalpy of activation (ΔH) and entropy of activation (ΔS) were calculated and discussed. Results showed that the values of E and ΔH of Al2024 are lower than copper. This indicates that the corrosion reaction for aluminum alloy need lower energy to occur compared to copper. ZRA result shows that aluminum is the sacrificial anode when coupled with copper in 1.0 M nitric acid solution.

Keywords: Galvanic corrosion; thermodynamic parameters; ZRA; copper; aluminum

1. INTRODUCTION

Aluminum is used excessively in the modern world, and the uses of the metal are extremely diverse due to its many unusual combinations of properties. Applications for aluminum include ship hulls, piers, tank interiors, offshore structure, submerged pipelines, piling [1]. Copper is a very widely used material for its excellent electrical and thermal conductivities in many industrial applications [2-4]. There are a lot of pipes, tanks, valves, tubes in condensers and heat exchangers are made from copper in the industries. Nitric acid is commonly used as a strong oxidizing agent. In industry, nitric acid plays a significant role in the manufacture of various products such as explosives like trinitrotoluene (T.N.T.) nitro glycerin, gun cotton and ammonal, fertilizers such as calcium nitrate, and ammonium nitrate, nitrate salts such as calcium nitrate, silver nitrate, ammonium nitrate, dyes,

perfumes from coal tar products, sulfuric acid by Lead Chamber process. Besides that, nitric acid is widely used in the purification of silver, gold and platinum, etching designs on copper, brass, and bronze ware [5]. Direct contact between different metals occurs commonly in equipment that transmits oilfield production liquids. Downhole and surface pump assemblies frequently combine copper alloys, carbon steels, aluminum alloy, low-alloy steels, stainless steels (SS), and steels plated by other metals. Sometimes, these galvanic couples lead to a corrosion problem [6].

Farrell [7] evaluated the potential galvanic coupling of Cu and Al in contact with several PCMs. This choice of these materials was due to the usual combination of both in heat exchangers. The main data reported show that aluminum alloy 2024 corrodes in the form of pitting with all the evaluated PCMs, and that the largest corrosion occurs when aluminum is coupled with copper in the acetate PCM.

In this study, the corrosion of aluminum alloy (Al2024) and copper was studied individually in 1.0 M HNO_3 solution at 30, 40, 50, 60 °C using electrochemical impedance spectroscopy (EIS) and potentiodynamic polarization (PDP) methods. Corrosion kinetic parameters were calculated and discussed. The galvanic corrosion of coupled metals was also investigated using zero resistance ammetry (ZRA) method.

2. EXPERIMENTAL WORK

The working electrodes consisted of Al2024 and copper with active surface areas of 3 cm². The composition of Al2024 was (by weight) 3.8% Cu, 0.1% Cr, 0.5% Fe, 1.2% Mg, 0.3% Mn, 0.5% Si, 0.15% Ti and 0.25% Zn, and the balance was Al. The copper electrode was 99.994% pure. The specimens were cleaned according to ASTM standard G1-03 [8]. All measurements were carried out in stagnant, non-aerated 1.0 M HNO_3 acid solutions. A Gamry Potentiostat/Galvanostat/ZRA (Ref. 600) was used to perform the corrosion tests. A three-electrode corrosion cell, with working electrode, graphite counter electrode and saturated calomel electrode (SCE) as the reference electrode, was connected to the Gamry Potentiostat/Galvanostat/ZRA instrument for corrosion measurements. The temperature of the corrosion cell was thermostatically controlled.

The electrochemical cell was allowed to stabilize before performing the electrochemical measurements. The EIS measurements for the Al2024 electrode were performed at the frequencies between 10 kHz and 0.1 Hz, with a signal potential perturbation amplitude of 10 mV. For the copper electrode the frequencies were between 10 kHz to 0.01 Hz, with a signal potential perturbation amplitude of 10 mV. The impedance data were fitted to appropriate equivalent circuits using Gamry Echem Analyst software. The potentiodynamic current-potential curves were obtained by changing the working electrode potential automatically from -200 to 200 mV versus SCE with a scan rate of 0.5 mV s⁻¹. For the galvanic corrosion measurements, the galvanic current density (I_g) and galvanic potential (E_g) were recorded simultaneously as a function of time using the Gamry Potentiostat/Galvanostat/ZRA instrument and applying a zero potential against the galvanic cell. Al2024 and copper electrodes were installed as a bimetallic shaft (Pine Instruments, Inc, USA) and were immersed in 1.0 M HCl solution for approximately 100 min.

3. RESULTS AND DISCUSSION

3.1. Electrochemical impedance spectroscopy (EIS) measurements

3.1.1. Aluminum alloy (Al2024)

Nyquist plots for Al2024 in 1.0 M nitric acid for different temperatures are shown in Fig. 1. In the recorded Nyquist plots, it is clearly seen that the impedance is decrease with increasing temperature.

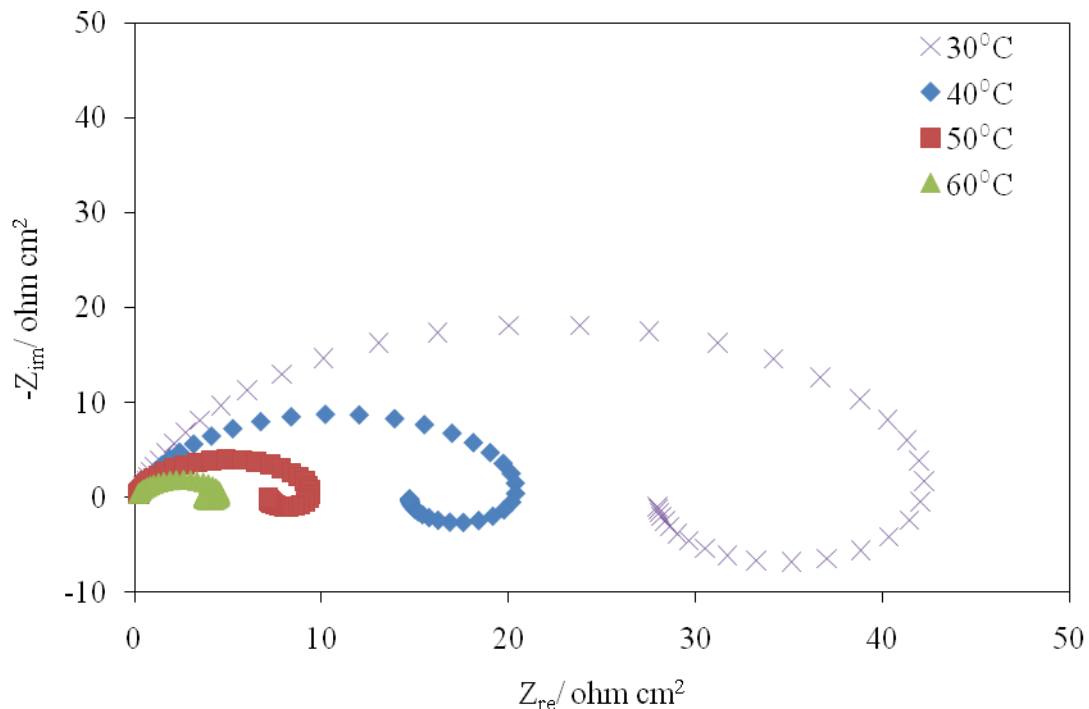


Figure 1. Nyquist plots for Al2024 in 1.0 M nitric acid solution at different temperatures

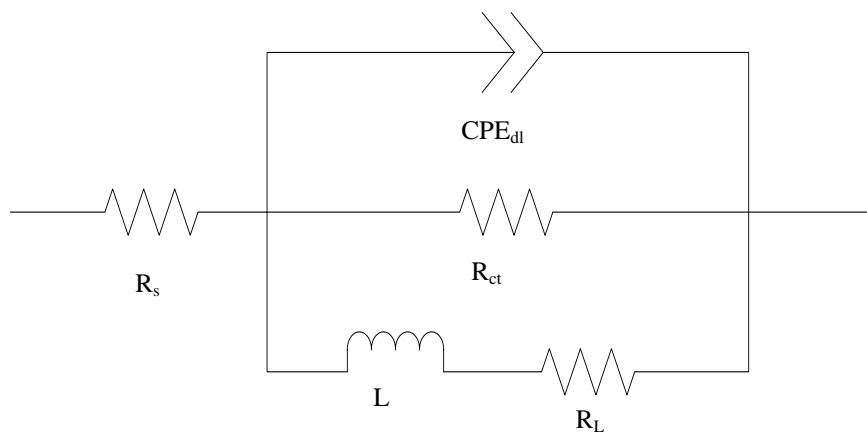


Figure 2. Equivalent Circuit Model used to fit the experimental data for Al2024 in 1.0 M nitric acid solution at different temperatures

The Nyquist plot is characterized by semicircular capacitive loop at intermediate frequencies and followed by inductive loop at low frequencies. Musa et al. [3] have reported the similar literature result for aluminum in nitric acid. The relaxation process in the aluminum oxide film on the surface of aluminum cause the capacitive loop at intermediate frequency whereas the redissolved of passivized surface cause the inductive loop at low frequency. The equivalent circuit model used to fit the system is shown in Fig. 2. The circuit consists of solution resistor (R_s) which is in series with constant phase element (CPE) which represent the capacitance of the double-layer. CPE is connected parallel with charge transfer resistance (R_{ct}). Layer resistance connected in series with inductor (L). CPE is defined in impedance representation as

$$Z(\omega) = Z_0 \cdot j\omega^{-\alpha} \tag{1}$$

where Z_0 is the CPE constant, ω is the angular frequency in rad/s, $j^2 = -1$ is the imaginary numbers, and α is the CPE exponent [3].

Table 1. Fitted impedance parameters of Al2024 in 1.0 M HNO₃ at different temperatures

Temperature (°C)	R_s (ohms cm ²)	L (H cm ²)	R_{ct} (ohms cm ²)	CPE_{dl}		C_{dl} (μF cm ⁻²)
				$Y_0 \times 10^6$ (S s ^α cm ⁻²)	α	
30	0.9774	48.78	126.30	0.456	0.90	6.489
40	0.5031	6.66	63.99	0.475	0.88	2.453
50	0.3516	1.62	29.64	0.613	0.86	1.024
60	0.2984	0.39	14.78	1.069	0.82	0.465

The fitted impedance parameters are shown in Table 1. The values of R_{ct} are decrease with increasing in solution temperature. Generally, corrosion rate of the metals is increase with increasing in solution temperature therefore the charge transfer resistance is decrease with increasing in solution temperature.

3.1.2. Copper

Nyquist plots for copper in 1.0 M nitric acid for different temperatures are shown in Fig. 3. At high frequency values, the Nyquist plot presents a depressed semicircle. The high frequency semicircle is caused by the single time constant of charge transfer resistance, R_{ct} and the double layer capacitance, C_{dl} . In the region of high frequency, the electrode reaction is controlled by a charge transfer process. The similar literature results have been obtained for copper in nitric acid [6]. Nyquist plot for copper in 1.0 M nitric acid for 30 and 40°C present a depressed semicircle followed by a straight line portion in the low frequency region. The equivalent circuit model, as presented in Fig. 4(a) was used to fit the experimental impedance data for copper in 1.0 M nitric acid at 30, 50 and 60°C whereas Fig. 4(b) used to fit the data at 40°C. The equivalent circuit shown in Fig. 4(a) consists of solution resistance, R_s ,

which is in series with constant phase element (CPE_{dl}) and CPE_{dl} is in parallel with charge transfer resistance, R_{ct} . The circuit is then connected in series with CPE_L and parallel with layer resistance (R_L). The equivalent circuit in Fig. 4(b) was used for the EIS data displaying a capacitive loop. The corresponding fitting results are listed in Table 2. Results show that the charge transfer resistance, R_{ct} is decrease with increasing temperature.

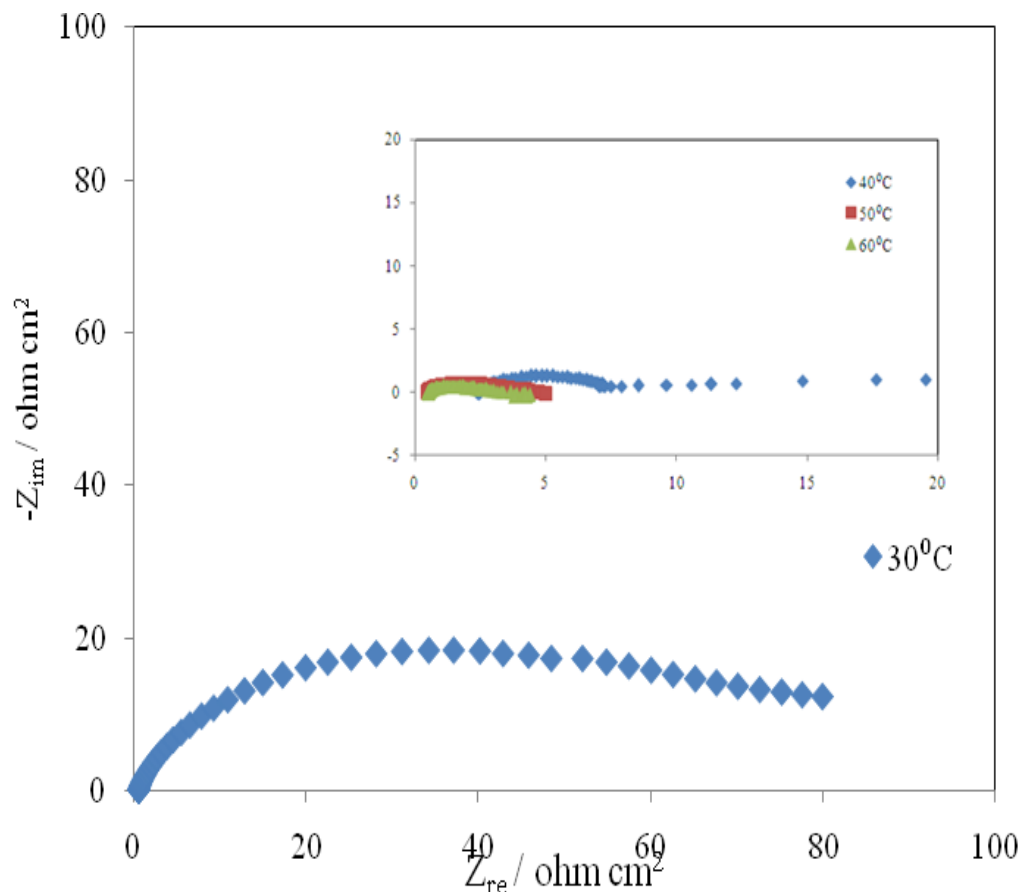


Figure 3. Nyquist plots for Cu in 1.0M nitric acid solution at different temperatures

Table 2. Fitted Impedance Parameters of Cu in 1.0M HNO₃ at different temperatures

Temperature (°C)	R _s (ohms cm ²)	CPE _{dl}		R _{ct} (ohms cm ²)	CPE _L		R _L (ohms cm ²)	C _{dl} (μF cm ⁻²)
30	4.6×10 ⁻¹	6.0×10 ⁻³	0.393	51.81	5.8×10 ⁻¹⁵	0.89	1.16×10 ⁻³	1.7×10 ⁴
40	1.15×10 ⁻²	5.1×10 ⁻²	0.066	6.79	-	-	-	3.2×10 ⁻²
50	8.8×10 ⁻⁵	8.5×10 ⁻²	0.052	1.78	3.02×10 ⁻³	0.62	30.4×10 ⁻⁹	6.1×10 ⁻¹¹
60	2.16×10 ⁻⁶	8.9×10 ⁻²	0.014	1.39	0.02115	0.30	9.38×10 ⁻¹⁸	5.1×10 ⁻⁶⁰

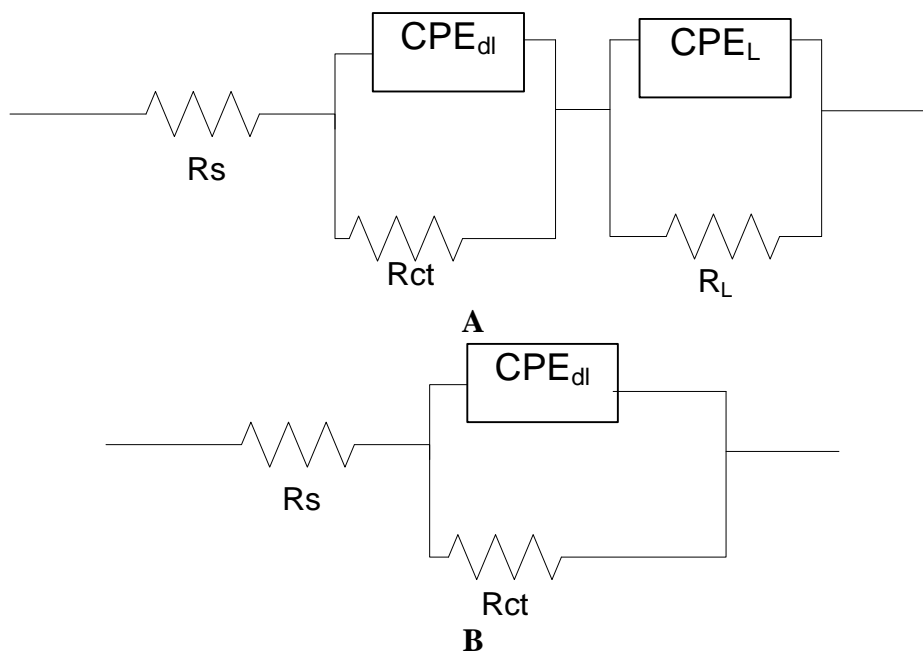


Figure 4 (a). Equivalent Circuit Modal used to fit the experimental data for Cu in 1.0 M nitric acid solution at 30, 50 and 60°C (b) Equivalent Circuit Modal used to fit the experimental data for Cu in 1.0 M nitric acid solution at 40°C

3.2. Potentiodynamic polarization (PDP) measurements

3.2.1. Aluminum alloy (Al2024)

Potentiodynamic polarization curves for aluminum alloy in 1.0 M nitric acid solution at the studied temperatures are shown in Fig. 5.

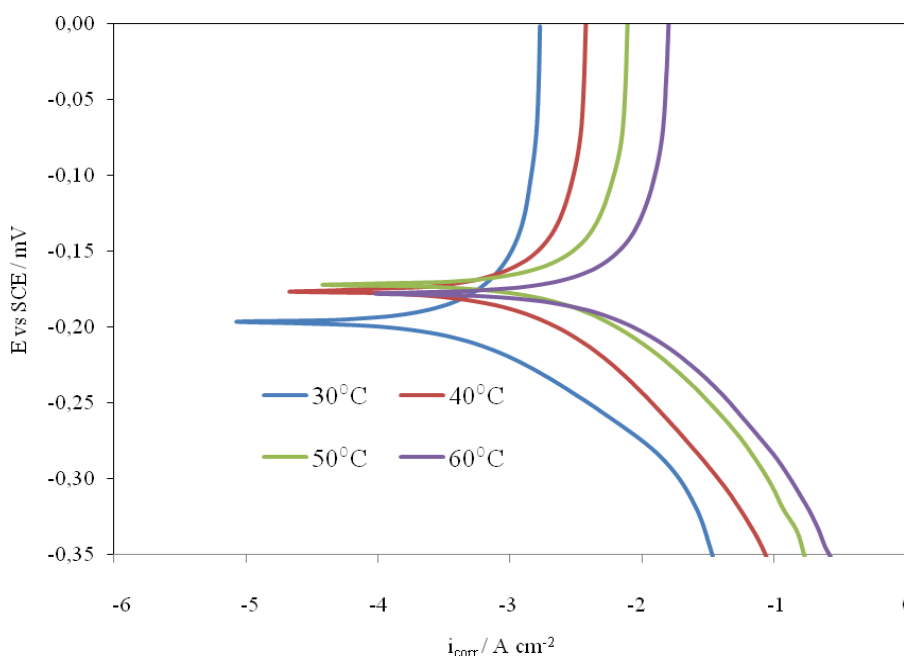


Figure 5. Potentiodynamic polarization curves for Al2024 in 1.0 M nitric acid solution at different temperatures

Table 3. Polarization parameters of Al2024 in 1.0 M HNO₃ at different temperatures

Temperature (°C)	β_a (V/decade)	β_c (V/decade)	I_{corr} (mA/cm ²)	$-E_{corr}$ (mV vs SCE)	Corrosion Rate (mmy)
30	0.816	0.097	1.23	197	4.35
40	0.176	0.075	1.75	176	6.187
50	0.853	0.083	5.85	171	20.71
60	0.146	0.065	6.10	177	21.58

The polarization parameters including the anodic (β_a) and cathodic (β_c) Tafel constants, corrosion current densities (i_{corr}) and corrosion potential (E_{corr}) are listed in Table 3. These values were calculated from the Tafel fit routine provided by Gamry Echem. Analyst software. This routine uses a non-linear chi-squared minimization to fit the data to the Stern-Geary equation which shown in Eq. 2.

$$i_{corr} = \frac{1}{2.303} \left(\frac{\beta_a \beta_c}{\beta_a + \beta_c} \right) \frac{1}{R_{ct}} \tag{2}$$

Corrosion of aluminum in aqueous solution has been reported to depend on the concentration of anions in solution [6].

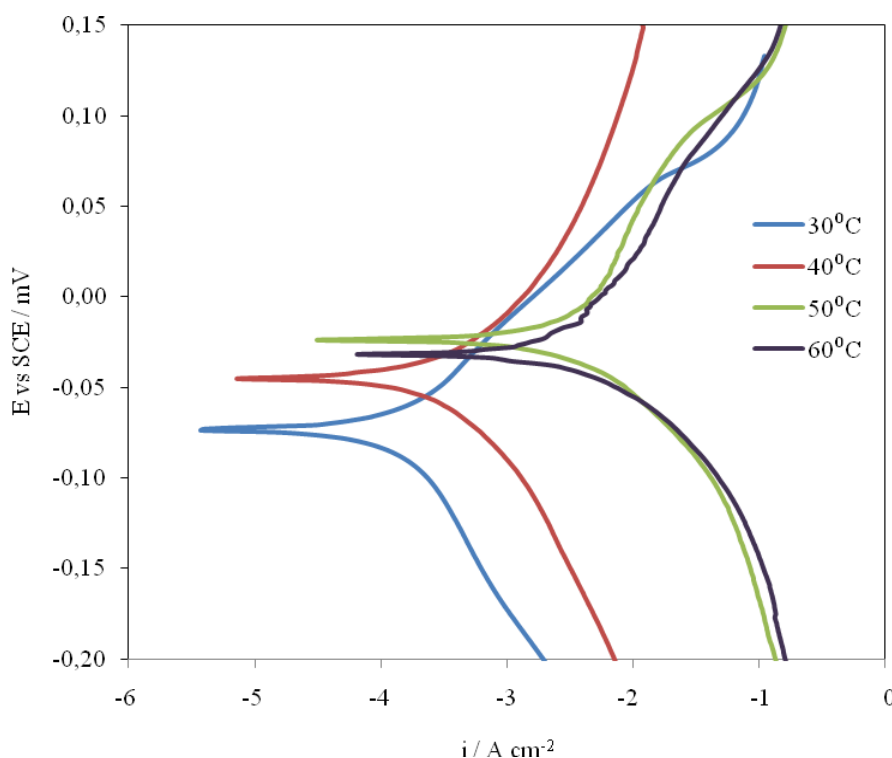
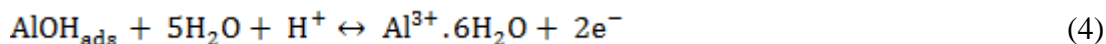


Figure 6. Potentiodynamic polarization curves for copper in 1.0 M nitric acid solution at different temperatures

The anodic polarization of aluminum in 1.0 M HNO₃ solution is described by dissolution of aluminum metal. The mechanism for the dissolution of aluminum in nitric acid was reported by Foley and Nguyen [7]



The controlling step in the metal dissolution is the complexation reaction between the hydrated cation and the anion which shown in Eq. (6). The soluble complex ion formed increases the metal dissolution rate which depends on the nitric acid concentration. The corrosion current density is found to increase with temperature as shown in Table 3. It can be seen from Fig. 6 that the polarization curve is shift to higher current density with increasing in solution temperature. Table 3 shows that the values of corrosion potential (E_{corr}) were slightly changed while the values of corrosion current densities (i_{corr}) of aluminum were increased with increasing in solution temperature.

3.2.2. Copper

The anodic and cathodic polarization curves of copper in 1.0 M HNO₃ solution for different temperatures are shown in Fig. 6.

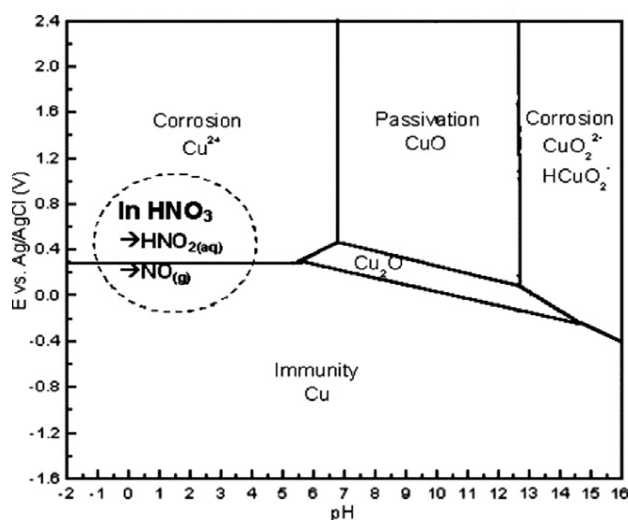


Figure 7. Potential–pH equilibrium diagram for the system, copper–water, at 25 ± 1 °C. The dashed regions and the equilibrium components corresponding to the Pourbaix diagram in HNO₃ solution [6].

The polarization parameters including the anodic (β_a) and cathodic (β_c) Tafel constants, corrosion current densities (i_{corr}) and corrosion potential (E_{corr}) are listed in Table 4.

Table 4. Polarization parameters of Copper in 1.0 M HNO₃ at different temperatures

Temperature (°C)	β_a (V/decade)	β_c (V/decade)	I_{corr} (mA/cm ²)	$-E_{corr}$ (mV vs SCE)	Corrosion Rate (mmy)
30	0.086	0.157	0.23	73.6	0.90
40	0.189	1.278	1.66	44.4	6.42
50	0.136	0.046	3.64	23.3	14.12
60	0.139	0.053	4.28	31.7	16.57

The parameters were calculated using same method as mentioned earlier. Nitric acid is a strong copper oxidizer which can attack copper rapidly. Besides that, the potentiodynamic polarization curves in Fig. 6 show that there is no steep slope in the anodic range. This means that there are no passive films formed on the copper surface. Thus, copper may directly dissolve in 1.0 M nitric acid solutions [6]. The Pourbaix diagram for copper–water is shown in Fig. 7. The Pourbaix diagram shows that copper is corroded to become copper ion, Cu²⁺ in nitric acid solution. In addition, there is no oxide film is formed to protect the surface from corrosion. Thus, copper dissolution is the dominant reaction in nitric acid solutions The electrochemical reactions for copper in HNO₃ solution can be described as follow:

Anodic reaction:



Cathodic reactions:

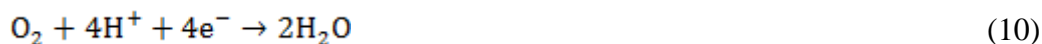


Table 4 revealed a slightly change in E_{corr} while the corrosion current density is increase with increasing in solution temperature.

3.3. Corrosion kinetic parameters

In general, the rate of most chemical reactions increases with temperature following Arrhenius equation [8]. In the case of the electrochemical reactions, temperature favors the kinetics of corrosion

reactions and more specifically, the anodic dissolution of the metal. The activation energy of the corrosion process can be obtained from the plots of Arrhenius according to the following equation:

$$i_{\text{corr}} = Ae^{-E_a/RT} \quad (11)$$

where E_a is the activation energy of the process (J/mol), R is the universal gas constant (8.314 J/(mol.K)), T is the temperature (K) and A is a constant. Taking the logarithm of the Arrhenius equation yields:

$$\text{Log } i_{\text{corr}} = \log(A) - \frac{E_a}{2.303RT} \quad (12)$$

the value of activation energy of corrosion can be determined from the slope of $\text{Log } (i_{\text{corr}})$ versus $1/T$ plots.

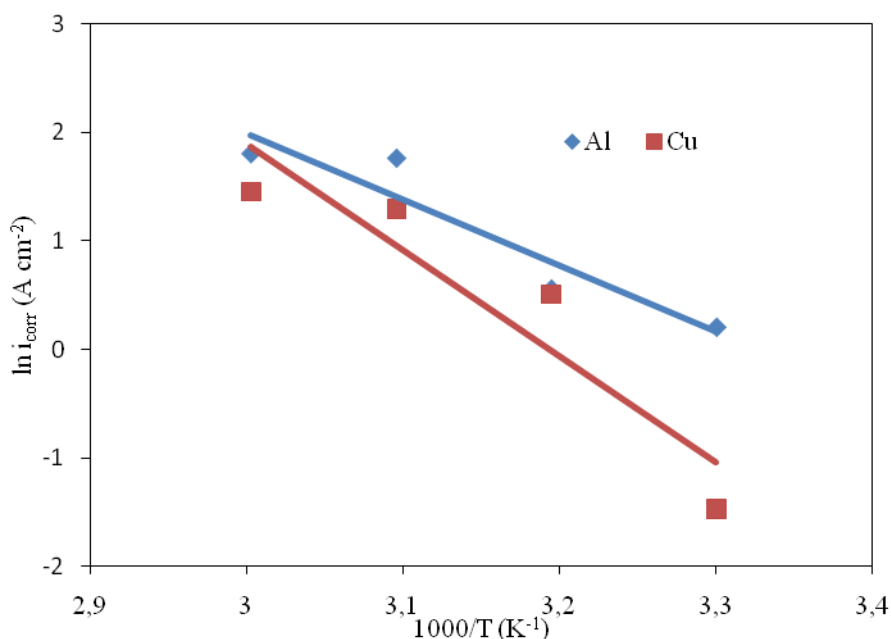


Figure 8. Arrhenius plots for aluminum and copper in 1.0 M nitric acid solution

Corrosion current density values of aluminum and copper which were obtained previously from potentiodynamic polarization measurements were plotted according to Eq. 12 in Fig. 8. From the gradient of the plotted curve, the calculated E_a for aluminum and copper are 50.54 and 81.06 kJ/mol, respectively. The activation energy of an electrochemical process refers to the energy level that must be overcome by one electron in the exchange through the interphase between electrode and electrolyte. In this way, low E_a values indicate high corrosion rates. Moreover, Arrhenius equation indicates that the greater the dependence of the corrosion rate on temperature, the higher the E_a values [8]. The highest E_a value was obtained for copper. This could be expected because the corrosion current density

of copper is lower than that of aluminum at different temperatures. The Arrhenius theory shares some similarities with collision theory. The reaction is occurring when molecules collide with each other. There is a basic assumption that made in the transition state theory that is the molecular system which in the direction of products after cross the transition state cannot turn around to form reactants anymore. A transition state complex is decays to products after forming the high energy. The mathematical form of transition state theory is written as:

$$i_{\text{corr}} = \left(\frac{RT}{Nh}\right) \exp\left(-\frac{\Delta H}{RT}\right) \exp\left(\frac{\Delta S}{R}\right) \tag{13}$$

where ΔH is enthalpy of activation, ΔS is the entropy of activation, N is Avogadro number (6.022×10^{23} molecule mol⁻¹) and h is the Plank's constant (6.626×10^{-34} J sec mol⁻¹)

In order to find the values of enthalpy and entropy of activations, Eq. 13 can be rearranged in the form of straight line equation. The rearranged equation is:

$$\ln\left(\frac{i_{\text{corr}}}{T}\right) = \ln\left(\frac{R}{Nh}\right) + \frac{\Delta S}{R} - \frac{\Delta H}{RT} \tag{14}$$

The values of enthalpy and entropy of activation for both aluminum and copper corrosion in 1.0 M nitric acid can be evaluated from the slope and intercept of the curve of $\ln\left(\frac{i_{\text{corr}}}{T}\right)$ versus $\frac{1}{T}$ as shown in Fig. 9.

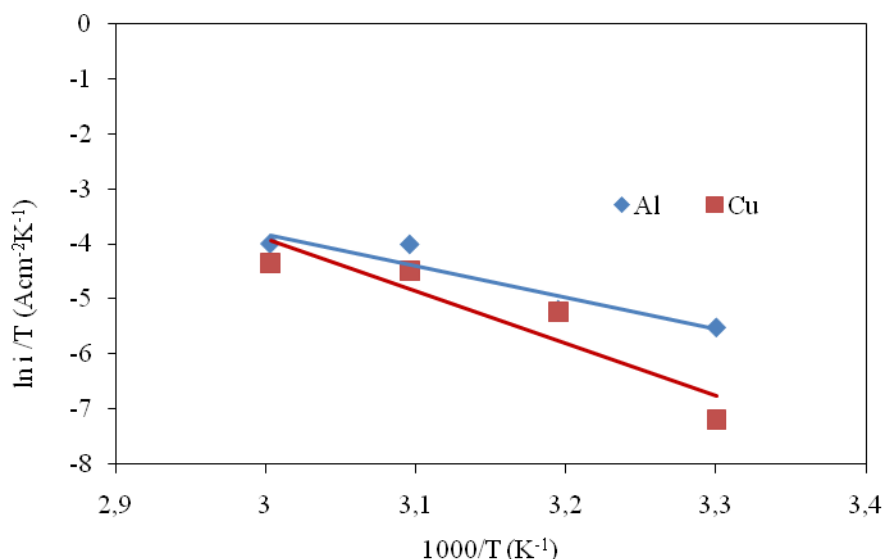


Figure 9. Transition State Plot for aluminum and copper in 1.0 M nitric acid solution

The values of enthalpy and entropy of activation for both aluminum and copper corrosion were tabulated in Table 5. The value of ΔH for aluminum alloy (47.91 kJ/mol) is lower than copper (78.43 kJ/mol) at 1.0 M nitric acid solution. This indicates that the corrosion reaction for aluminum alloy need

lower energy to occur compared to copper. The energy barrier of corrosion reaction for aluminum is lower than copper and the transition state complex can be formed faster for the corrosion reaction for aluminum.

Table 5. Corrosion kinetic parameters for aluminum and copper in 1.0 M nitric acid solution

Metal	Arhenius Equation	Transition State Equation	
	E (kJ/mol)	ΔH (kJ/mol)	ΔS (J/mol.K)
Aluminum alloy	50.54	47.91	-85.63
Copper	81.06	78.43	5.16

The positive values of ΔH indicate that the dissolution of aluminum and copper are endothermic process. The value of ΔS for aluminum alloy is negative (-85.63 J/mol.K) whereas for copper is positive (5.16 J/mol.K). According to Aprael et al. [4] the corrosion of metals in acidic solution is cathodically controlled by the hydrogen evolution reactions which occur in two steps:



The rate-determining step for the hydrogen evolution reaction is the recombination of adsorbed hydrogen atoms to form hydrogen molecules as written in Eq. 18. For aluminum, the entropy of activation has a negative value as the activated complex is more orderly relative to the initial state. On the other hand, the entropy of activation for copper is positive value as the transition state of the rate determining recombination step represent less orderly arrangement relative to the initial state.

3.4. Zero resistance ammetry (ZRA)

The galvanic current density, I_g and galvanic potential, E_g for the coupled of aluminum and copper is shown in Fig. 10. The couple of aluminum and copper was immersed in 1.0 M nitric acid solution for two hours. Since the open circuit potential of copper (-38 mV/SCE) is higher than the open circuit potential of aluminum (-182 mV/SCE), the current is flow from copper to aluminum [9]. This is because the electrode potential of aluminum is lower than copper before coupling, therefore, aluminum is the anode and copper is the cathode. After immersed in nitric acid solution for two hours, aluminum formed a protective oxide film and become the sacrificial anode, thus, copper is protected.

It can be seen from Fig. 10 that the current is decreased from 600 mA at the beginning over 10 minutes and then decrease. The decrease of the current is due to the formation of passive oxide layer [3]. There is a sharp variation of the current at 40 minutes, this is due to the diffusion of the electrolyte into the inner oxide layers and wet the entire surface film [6]. There is further decrease of current at 40 minutes; this is due to the hinder dissolution of metal by the passive oxide formed. When the steady

state condition was reached, the current tends towards 35 mA. The current is almost constant from 80 minutes to 130 minutes which due to stabilization of passive oxide layer [9].

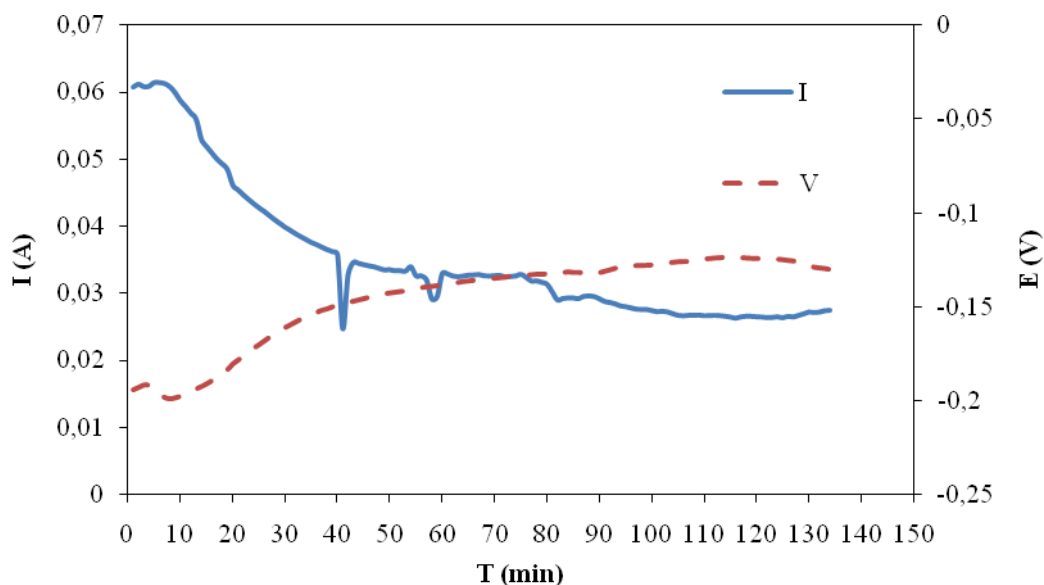


Figure 10. Galvanic Corrosion of Al2024 and Copper in 1.0 M nitric acid solution at 30°C

4. CONCLUSION

Corrosion of Al2024 and copper in 1.0 M nitric acid solution at different temperature was studied using electrochemical impedance spectroscopy (EIS) and potentiodynamic polarization methods. Zero resistance ammetry (ZRA) was used for the measurements of galvanic corrosion of aluminum Al2024 and copper. Results show that the current density is increase with temperature. Results from the applications of Arrhenius equation and transition state theory showed that the activation energy of Al2024 is lower than copper. The value of ΔH for aluminum alloy (47.91 kJ/mol) is lower than copper (78.43 kJ/mol) at 1.0 M nitric acid solution. The value of ΔS for aluminum alloy is negative (-85.63 J/mol.K) whereas for copper is positive (5.16 J/mol.K). The energy barrier of corrosion reaction for aluminum is lower than copper and the transition state complex can be formed faster for the corrosion reaction for aluminum.

ACKNOWLEDGMENT

This work was supported by Universiti Kebangsaan Malaysia (No. UKM-GGPM-NBT-037-2011) which is gratefully acknowledged.

References

1. T. A. Markley, M. Forsyth and A. E. Hughes, *Electrochimi. Act.* 52 (2007)4024

2. K. Barouni, L. Bazzi, R. Salghi, M. Mihit, B. Hammouti, A. Albourine and S. El Issami, *Materials Letters* 62 (2008) 3325
3. A. Y. Musa, A. B. Mohamad, A. A. H. Kadhum and Y. B. A. Tabal, *J. Mater. Eng. Perf.* 20 (2011) 394
4. A. Y. Musa, A. A. H. Kadhum, A. B. Mohamad and M. S. Takriff, *Inter. J. Surf. Sci. Eng.* 5(2011) 226
5. A. A. Khadom, A. S. Yaro, A. A. H. Kadum, A. S. AlTaie and A. Y. Musa, *Amer. J. Appl. Sci.* 6 (2009)1403
6. R. L. Martin, *Corrosion*, 51(1995)482
7. A J. Farrell, B. Norton and D.M. Kennedy, *J. Mater. Process. Tech.* 175 (2006)198
8. ASTM G1-3, Standard Practice for Preparing, Cleaning, and Evaluating Corrosion Test Specimens.
9. K.F. Khaled, *Corro. Sci.* 52 (2010) 2905
10. R.T. Foley and T.H. Nguyen, *J. Electrochem. Soc.* 129(1982) 464
11. R. Sanchez-Tovar, M.T. Montanes and J. Garcia-Anton, *Corros. Sci.* 52 (2010) 722
12. Ahmad, Z. 2006. *Principles of Corrosion Engineering and Corrosion Control*. USA: Butterworth-Heinemann.